Control of the attosecond synchronization of XUV radiation with phase-optimized mirrors

Charles Bourassin-Bouchet, Z. Diveki, Sébastien De Rossi, E. English, Evgueni Meltchakov, O. Gobert, D. Guénot, Bertrand Carre, Franck Delmotte, Pascal Salières, et al.

Control of the attosecond synchronization of XUV radiation with phase-optimized mirrors

C. Bourassin-Bouchet,[1,*] Z. Diveki,[2] S. de Rossi,[1] E. English,[2] E. Meltchakov,[1] O. Gobert,[2] D. Guénot,[2] B. Carré,[2] F. Delmotte,[1] P. Salières,[2] and T. Ruchon[2]

[1]*Laboratoire Charles Fabry, Institut d'Optique, Université Paris-Sud, CNRS, 2 Avenue Augustin Fresnel, 91127 Palaiseau, France*

[2]*CEA-Saclay, IRAMIS, Service des Photons, Atomes et Molécules, 91191 Gif-sur-Yvette, France*

[*]*charles.bourassin-bouchet@institutoptique.fr*

Abstract: We report on the advanced amplitude and phase control of attosecond radiation allowed by specifically-designed multilayer XUV mirrors. We first demonstrate that such mirrors can compensate for the intrinsic chirp of the attosecond emission over a large bandwidth of more than 20 eV. We then show that their combination with metallic foils introduces a third-order dispersion that is adjustable through the mirror's incidence angle. This results in a controllable beating allowing the radiation to be shaped from a single to a series of sub-100 as pulses.

OCIS codes: (120.5050) Phase measurement; (230.4170) Multilayers; (320.5540) Pulse shaping; (340.7480) X-rays, soft x-rays, extreme ultraviolet (EUV).

References and links

1. F. Krausz and M. Ivanov, "Attosecond physics," Rev. Mod. Phys. **81,** 163–234 (2009).
2. C. Froehly, B. Colombeau, and M. Vampouille, "Shaping and analysis of picosecond light pulses," Prog. Opt. **33,** 65–153 (1983).
3. P. Tournois, "Acousto-optic programmable dispersive filter for adaptive compensation of group delay time dispersion in laser systems," Opt. Commun. **140,** 245–249 (1997).
4. M. Ferray, A. L'Huillier, X. F. Li, L. A. Lompre, G. Mainfray, and C. Manus, "Multiple-harmonic conversion of 1064 nm radiation in rare gases," J. Phys. B **21,** L31–L35 (1988).
5. A. McPherson, G. Gibson, H. Jara, U. Johann, T. S. Luk, I. A. McIntyre, K. Boyer, and C. K. Rhodes, "Studies of multiphoton production of vacuum-ultraviolet radiation in the rare gases," J. Opt. Soc. Am. B **4,** 595–601 (1987).
6. Y. Mairesse, A. de Bohan, L. J. Frasinski, H. Merdji, L. C. Dinu, P. Monchicourt, P. Breger, M. Kovacev, R. Taïeb, B. Carré, H. G. Muller, P. Agostini, and P. Salières, "Attosecond synchronization of high-harmonic soft x-rays," Science **302,** 1540–1543 (2003).
7. K. Varjú, Y. Mairesse, P. Agostini, P. Breger, B. Carré, L. J. Frasinski, E. Gustafsson, P. Johnsson, J. Mauritsson, H. Merdji, P. Monchicourt, A. L'Huillier, and P. Salières, "Reconstruction of attosecond pulse trains using an adiabatic phase expansion," Phys. Rev. Lett. **95,** 243901 (2005).
8. K. Varjú, Y. Mairesse, B. Carré, M. B. Gaarde, P. Johnsson, S. Kazamias, R. López-Martens, J. Mauritsson, K. J. Schafer, Ph. Balcou, A. L'Hullier, and P. Salières, "Frequency chirp of harmonic and attosecond pulses," J. Mod. Opt. **52,** 379 (2005).
9. J. Tate, T. Auguste, H. G. Muller, P. Salières, P. Agostini, and L. F. DiMauro, "Scaling of wave-packet dynamics in an intense midinfrared field," Phys. Rev. Lett. **98,** 013901 (2007).
10. W. Boutu, S. Haessler, H. Merdji, P. Breger, G. Waters, M. Stankiewicz, L. J. Frasinski, R. Taïeb, J. Caillat, A. Maquet, P. Monchicourt, B. Carré, and P. Salières, "Coherent control of attosecond emission from aligned molecules," Nat. Phys. **4,** 545–549 (2008).

#140608 - $15.00 USD Received 4 Jan 2011; revised 4 Feb 2011; accepted 5 Feb 2011; published 11 Feb 2011

11. X. Zhou, R. Lock, W. Li, N. Wagner, M. M. Murnane, and H. C. Kapteyn, "Molecular recollision interferometry in high harmonic generation," Phys. Rev. Lett. **100,** 073902 (2008).
12. T. Ruchon, C. P. Hauri, K. Varjú, E. Mansten, M. Swoboda, R. López-Martens, and A L'Huillier, "Macroscopic effects in attosecond pulse generation," New J. Phys. **10,** 025027 (2008).
13. K. T. Kim, C. M. Kim, M.-G. Baik, G. Umesh, and C. H. Nam, "Single sub-50-attosecond pulse generation from chirp-compensated harmonic radiation using material dispersion," Phys. Rev. A **69,** 051805 (2004).
14. R. López-Martens, K.Varjú, P. Johnsson, J. Mauritsson, Y. Mairesse, P. Salières, M. B. Gaarde, K. J. Schafer, A. Persson, S. Svanberg, C.-G. Wahlström, and A. L'Huillier, "Amplitude and phase control of attosecond light pulses," Phys. Rev. Lett. **94,** 033001 (2005).
15. E. Gustafsson, T. Ruchon, M. Swoboda, T. Remetter, E. Pourtal, R. López-Martens, Ph. Balcou, and A. L'Huillier, "Broadband attosecond pulse shaping," Opt. Lett. **32,** 1353–1355 (2007).
16. D. H. Ko, K. T. Kim, J. Park, J. Lee, and C. H. Nam, "Attosecond chirp compensation over broadband high-order harmonics to generate near transform-limited 63 as pulses," New J. Phys. **12,** 063008 (2010).
17. R. Szipocs, K. Ferencz, C. Spielmann, and F. Krausz, "Chirped multilayer coatings for broadband dispersion control in femtosecond lasers," Opt. Lett. **19,** 201–203 (1994).
18. A. Wonisch, T. Westerwalbesloh, W. Hachmann, N. Kabachnik, U. Kleineberg, and U. Heinzmann, "Aperiodic nanometer multilayer systems as optical key components for attosecond electron spectroscopy," Thin Solid Films **464-465,** 473–477 (2004).
19. A.-S. Morlens, Ph. Balcou, Ph. Zeitoun, C. Valentin, V. Laude, and S. Kazamias, "Compression of attosecond harmonic pulses by extreme-ultraviolet chirped mirrors," Opt. Lett. **30,** 1554–1556 (2005).
20. A.-S. Morlens, R. López-Martens, O. Boyko, Ph. Zeitoun, Ph. Balcou, K. Varjú, E. Gustafsson, T. Remetter, A. L'Huillier, S. Kazamias, J. Gautier, F. Delmotte, and M.-F. Ravet, "Design and characterization of extreme-ultraviolet broadband mirrors for attosecond science," Opt. Lett. **31,** 1558–1560 (2006).
21. E. Goulielmakis, M. Schultze, M. Hofstetter, V. S. Yakovlev, J. Gagnon, M. Uiberacker, A. L. Aquila, E. M. Gullikson, D. T. Attwood, R. Kienberger, F. Krausz, and U. Kleineberg, "Single-cycle nonlinear optics," Science **320,** 1614–1617 (2008).
22. S. Kirkpatrick, C. D. Gelatt, and M. P. Vecchi, "Optimization by simulated annealing," Science **220,** 671–680 (1983).
23. M. Yamamoto and T. Namioka, "Layer-by-layer design method for soft-x-ray multi layers," Appl. Opt. **31,** 1622–1630 (1992).
24. J. Gautier, F. Delmotte, M. Roulliay, F. Bridou, M.-F. Ravet, and A. Jérome, "Study of normal incidence of three-component multilayer mirrors in the range 20-40 nm," Appl. Opt. **44,** 384–390 (2005).
25. A. Aquila, F. Salmassi, and E. Gullikson, "Metrologies for the phase characterization of attosecond extreme ultraviolet optics," Opt. Lett. **33,** 455–457 (2008).
26. M. Suman, G. Monaco, M.-G. Pelizzo, D. L. Windt, and P. Nicolosi, "Realization and characterization of an XUV multilayer coating for attosecond pulses," Opt. Express **17,** 7922–7932 (2009).
27. S. Haessler, B. Fabre, J. Higuet, J. Caillat, T. Ruchon, P. Breger, B. Carré, E. Constant, A. Maquet, E. Mével, P. Salières, R. Taïeb, and Y. Mairesse, "Phase-resolved attosecond near-threshold photoionization of molecular nitrogen," Phys. Rev. A **80,** 011404 (2009).
28. S. Haessler, J. Caillat, W. Boutu, C. Giovanetti-Teixeira, T. Ruchon, T. Auguste, Z. Diveki, P. Breger, A. Maquet, B. Carré, R. Taïeb, and P. Salières, "Attosecond imaging of molecular electronic wavepackets," Nat. Phys. **6,** 200–206 (2010).
29. S. Zamith, J. Degert, S. Stock, B. de Beauvoir, V. Blanchet, M. A. Bouchene, and B. Girard , "Observation of coherent transients in ultrashort chirped excitation of an undamped two-level system," Phys. Rev. Lett. **87,** 033001 (2001).

1. Introduction

The advent of attosecond sources in the early 2000's has triggered a great deal of interest in many scientific communities ranging from atomic and molecular physics to surface science and chemistry [1]. However, although the demand is high, the generalization of these sources has been hampered by the difficulty to manipulate and control such ultrashort pulses. Indeed, this combines two difficulties: first, the pulses are centered in the XUV spectral range where absorption of most materials is high; second, they cover a huge spectral range (20 eV are needed to sustain 100 as pulses) making them very sensitive to any dispersive element that would distort the spectral phase and consequently the attosecond structure. It thus remains a challenge to control this radiation, shape it in the temporal and spectral domains, propagate it and deliver it on target without losing too much flux.

Current femtosecond infrared (IR) pulse shaping techniques, which are based either on a 4-f

#140608 - $15.00 USD Received 4 Jan 2011; revised 4 Feb 2011; accepted 5 Feb 2011; published 11 Feb 2011

zero dispersion optical delay line [2] or on an acousto-optic programmable dispersive filter [3], cannot be directly transposed in the XUV because of absorption. Therefore, the attosecond pulse control possibilities have been very limited so far. At the source, one may tailor their generation conditions, *i.e.* control the nonlinear interaction of the strong laser field with the gas target that results in High-order Harmonic Generation (HHG) [4, 5]. The laser parameters (intensity, wavelength) can be used to control the value of the intrinsic Group Delay Dispersion (GDD) and thus the chirp of the attosecond emission [6–9], but only in a limited range and without the possibility of introducing higher-order phase terms. The generating medium may also introduce spectral phase features, such as jumps or linear offsets, either on the molecular [10, 11] or macroscopic [12] levels, but with limited control over their position, amplitude and shape. Downstream, a post-control can be performed using dispersive media, such as metallic foils [13–15], plasmas [6] or atomic gases [16]. However, all these techniques suffer from a lack of versatility: they all depend on matching a spectrum to a given material. A more versatile control could be allowed by multiple interference effects as was performed in the IR region with chirped mirrors over sub-1 eV bandwidths [17]. Some steps have already been taken in that direction, through the design of XUV multilayer mirrors [18–20]. However no phase control over bandwidths of tens of eV has been demonstrated thus far, and chirped mirrors have not entered the attosecond realm. In this article, we report on the design and characterization of a toolset of mirrors that fulfill the four-fold objective: high reflectivity (10-20%) and phase control over 20-30 eV bandwidth, central energy of 50 eV where intense attosecond pulses can be generated, and 45° incidence to steer the beam. We show that such mirrors allow compensation for the intrinsic harmonic GDD, and thus compression of the attosecond pulses. Furthermore, their combination with standard metallic filters introduces third order dispersion opening new phase control opportunities. This allows for instance shaping the XUV pulse in the form of multi sub-100 as pulses. This attosecond beating is controllable through the mirrors' incidence angle.

2. Design of multilayer mirrors

The multiple beam interference effect occurring in the mirror structure provides a great deal of controls: one can adjust the alternating materials, thereby setting the Fresnel coefficients at each interface, the layer thicknesses, thereby setting the phase and group delays (GD), and the number of layers. Clearly, the greater the number of layers, the more comprehensive the control of the reflected field. However, the absorption of the materials in the 30-60 eV range limits the overall thickness of the stack to about 100 nm with approximately 10 layers (compared to up to 100 layers in the visible range). The first desirable function of a pulse shaper is the compensation of the intrinsic atto-chirp [6] in order to get Fourier-transform limited pulses. The second function would be to tailor the phase up to third order so as to design attosecond pulse shapes on demand, such as double or multiple pulses. All this, added to the targeted broad bandwidth, led us to include some extra liberty in the optimization process through the use of three materials, molybdenum, silicon and boron carbide, instead of the standard combination of two [21]. The optimization process used a metaheuristic, namely a simulated annealing algorithm [22] which took into account the behavior of the layers when they are stacked, such as their inter-diffusion and roughness. The evolution of the complex reflectivity of one optimized stack as one progresses through the mirror from the substrate is reported in Fig. 1 using the Yamamoto spiral [23].

The spiral actually turns around the Fresnel coefficients of the successive materials with an angular length and a variable radius determined by the layer thickness. In other words, the propagation through a layer modifies the accumulated phase and reflectivity at a given depth. It should be noted that Mo's reflectivity point is i) far away from the other materials' points, and

#140608 - $15.00 USD Received 4 Jan 2011; revised 4 Feb 2011; accepted 5 Feb 2011; published 11 Feb 2011

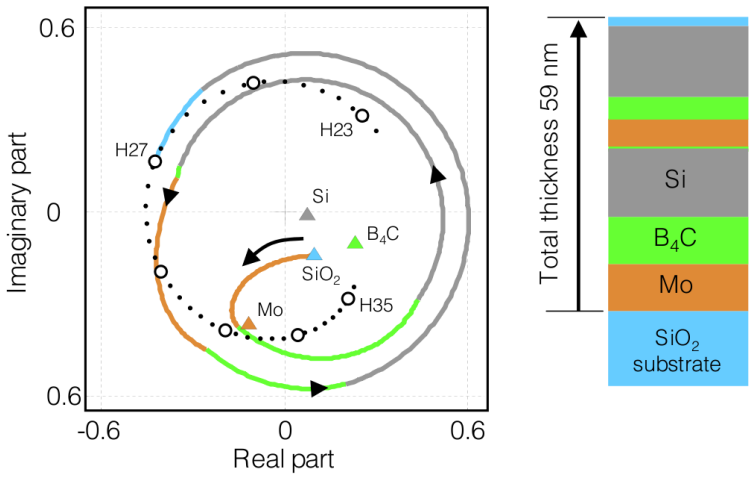

Fig. 1. Evolution of the complex reflectivity at an energy of 42 eV of the M_2 multilayer structure (shown on the right) as it is grown on the substrate (thick line colored depending on the layer). The Fresnel coefficients for the vacuum-material interfaces are shown in triangles. The end points of the spiral are displayed for 0.5 eV-spaced energies (dots) and for odd harmonic orders of an 800 nm laser (open circles).

ii) shifted along the imaginary axis due to high absorption. It thus plays a crucial role in shaping the phase and reflectivity of the stack. This representation also highlights the compromise that has to be made between the GDD and the reflectivity. Indeed when increasing the final silicon layer, the reflectivity becomes greater than 30% but the thickness of the layer is further increased to get the desired phase at this energy, even though it decreases the reflectivity to 20%. The spiral end points for harmonics 23-35 (36-54 eV) are reported in Fig. 1. The angular interval between two consecutive harmonics decreases with respect to the order, indicating a negative GDD of the mirror, as targeted in this case. Moreover the reflectivity remains high in this spectral range and does not vary much. It should be noted as well that the main effect is due to the mirror structure, *i.e.* interference effect, and not so much to the dispersion that slightly changes the position of the Fresnel coefficient points in Fig. 1 as the energy is varied. These simulations thus show that 3-material aperiodic mirrors have the capability to achieve our goal, *i.e.* broadband high reflectivity with controlled phase. To this aim, we optimized three mirrors on the 35-55 eV spectral range to get a constant GDD (M_1), with a theoretical reflectivity between 17% and 26%, or alternatively a -4200 as^2/rad (M_2) or a -8500 as^2/rad (M_3) GDD, with reflectivities greater than 11% on the optimized range. Their expected GDs calculated during the optimization are reported in Fig. 2 (Gray Lines). The mirrors coatings were deposited in a magnetron sputtering machine [24]. In order to guarantee a precision on the thicknesses better than 0.3 nm, we calibrated the deposition process with a grazing-incidence Cu-Kα reflectometer.

3. Setup and experimental results

The mirrors' reflectivity was characterized using the BEAR beamline at the ELETTRA synchrotron. For all three mirrors, the measured reflectivity was close to the calculated one, as exemplified in Fig. 2(d) for mirror M_2. The measurement of the mirrors' group delay is a much more difficult task that has become possible only recently, using either an indirect [25, 26] or

#140608 - $15.00 USD Received 4 Jan 2011; revised 4 Feb 2011; accepted 5 Feb 2011; published 11 Feb 2011

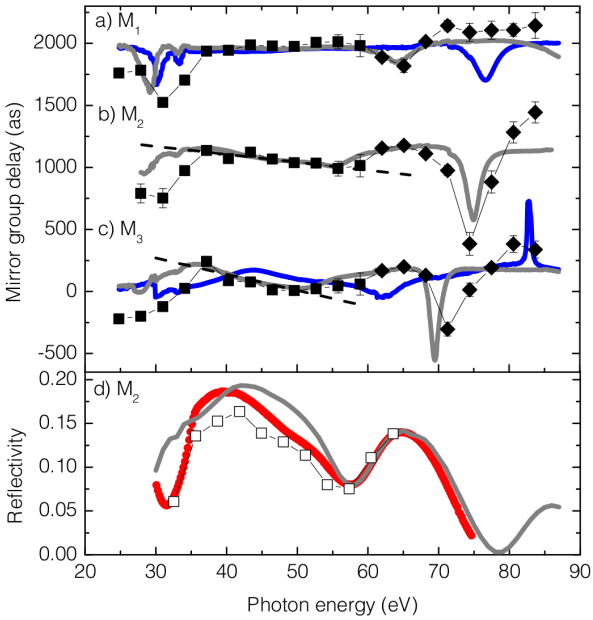

Fig. 2. Group delay (a-c) and reflectivity (d) of designed multilayer mirrors. In (a-c), the simulated GDs are plotted for 42° incidence (gray lines) and also for 52.5° in the case of M_1 and M_3 (blue lines). The GDs measured at 42° are reported in black squares (diamonds) when the experimental (extrapolated) reference was used. Dashed lines show linear fits performed over the optimized 35-55 eV range. The curves were vertically shifted for visibility; the GD absolute values were not measured in the experiment. In (d), the reflectivity of M_2 is plotted as a typical case: simulated (gray line), and measured reflectivity using HHG (open squares) and synchrotron radiation (red dots).

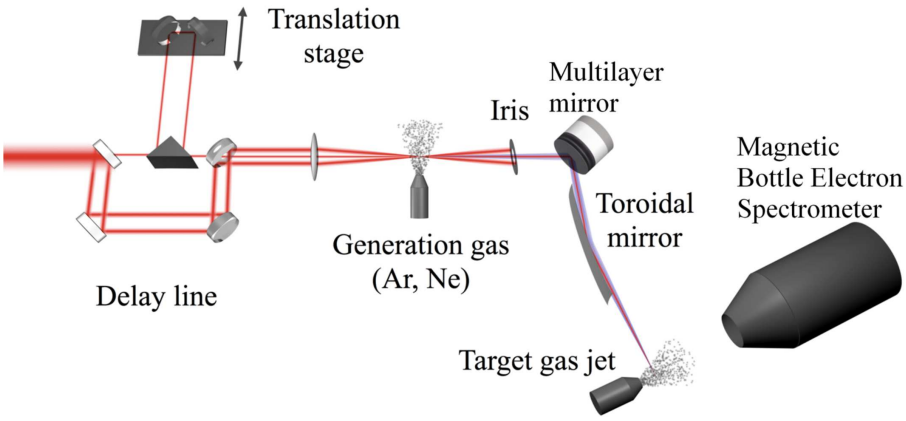

Fig. 3. Experimental setup on the attosecond beamline for the mirrors group delay characterization.

#140608 - $15.00 USD Received 4 Jan 2011; revised 4 Feb 2011; accepted 5 Feb 2011; published 11 Feb 2011

a direct [20] technique. The latter is very demanding since it requires both a broadband coherent XUV source and a group delay characterization setup. To do so, we used the attosecond beamline in CEA-Saclay, as described in Fig. 3. The 20 Hz, 50 fs, 800 nm LUCA laser beam first goes through a drilled-mirror-based interferometer which produces two beams of complementary shapes: one is ring-shaped and performs the high harmonic generation while the other, of much lower energy, is plain and provides the dressing beam for the RABITT measurement. Their relative delay can be finely adjusted by a piezoelectric delay stage. From the focusing lens on, the setup is placed under vacuum. The harmonics are generated in Ar or Ne gas jets which come out of a nozzle controlled by a piezoelectric crystal. To get rid of the intense generating beam, an iris is set after the gas jet. Its opening size is small enough to cut out the annular generating beam but large enough to let through the XUV radiation and the dressing beam. Both beams are then reflected off either the multilayer mirror or a reference silver mirror set at 42° and finally focused by a toroidal mirror at grazing incidence angle in the target gas (Ne). The electrons produced through two-photon XUV+IR photoionization are detected in a time-of-flight magnetic bottle electron spectrometer. The compactness of the setup results in a high stability but excludes placing any full metallic foil (like an aluminum filter for spectral selection) that would also block the infrared dressing beam used for the RABITT measurement. The RABITT temporal characterization technique [20], as opposed to the photocurrent technique [25, 26], is very effective in this spectral range at this incidence angle and has proven to be extremely sensitive to phase jumps [27, 28]. We first calibrated the reference mirror by comparison with "direct" measurements involving only grazing incidence reflections: it induces a +5300 as^2/rad GDD that adds to the intrinsic +6300 as^2/rad GDD of the neon attosecond emission. This was attributed to a hydrocarbon layer adsorbed on the mirror. Then, comparing the GDs measured on a beam reflected off a given multilayer mirror and off the reference silver mirror, we obtained the GDs reported in Fig. 2(a-c). The overall agreement with the simulations is excellent for the three mirrors: in the optimized 35-55 eV range, the XUV light can be reflected either with no phase distortion (M_1), or alternatively with a -4200 as2/rad (M_2) or a -8500 as2/rad (M_3) GDD. To illustrate this point, we plot in Fig. 4 the amplitudes and group delays of the harmonics reflected off M_2 and off the silver mirror. As expected, M_2 efficiently compensates for the intrinsic GDD of the harmonics, giving a flat GD in the 35-55 eV range.

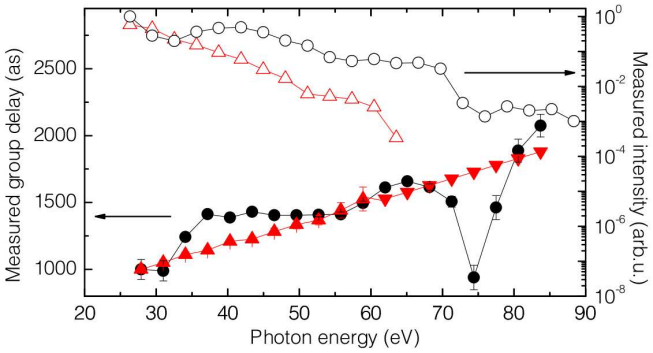

Fig. 4. Spectral intensity (open symbols) and GD (filled symbols) measured in the detection region after reflection off the Ag reference mirror (up triangles) and off M_2 (circles). The Ag low reflectivity above 65 eV prevented measurement of the GD. It was thus linearly extrapolated following [6] (down triangles): indeed the intrinsic harmonic GD was shown to vary linearly with harmonic order in the plateau region. Both GD curves are shifted to get the GD of sideband 18 (28 eV) at 1000 as.

#140608 - $15.00 USD Received 4 Jan 2011; revised 4 Feb 2011; accepted 5 Feb 2011; published 11 Feb 2011

4. Temporal reconstruction and discussion

As explained in the setup description, the RABITT version used in our measurements allows a broadband spectral characterization of the XUV radiation but is not compatible with spectral filtering. However, using i) tabulated values for the complex transmission of metallic foils, and ii) the measured spectral amplitudes and group delays, we can reconstruct reliably by Fourier transform the shape of the resulting attosecond pulses. First, in order to evidence the different effects generated by the mirrors on the attosecond pulse structure, we introduced numerically an amplitude filter. It was chosen to have a square shape, encompassing the common spectral range of measurements of all mirrors, namely 32.5-63.5 eV. The results are displayed in Fig. 5(a). The 135 and 123 as-long pulses obtained after reflection off M_2 and M_3 respectively are twice as short, and five times more intense than the one reflected off the reference mirror. As expected, mirror M_1 which does not compensate for the intrinsic chirp, gives a significantly different pulse shape and duration mainly due to the remaining GD of the radiation. This enlightens the crucial effect of the phase control achieved with M_2 and M_3. Note that for M_2 (resp. M_3), by adding a few harmonic orders on both sides of the optimized 35-55 eV range where the GD smoothly deviates from the constant value, a pulse duration close to the Fourier transform limit of 124 as (resp. 115 as) is still obtained.

Second, Fig. 5(b) shows the pulse profiles that would be obtained in a realistic attosecond experiment where the harmonic radiation would be spectrally filtered using a standard 250 nm-thick aluminum filter. Its complex transmission is calculated from tabulated indices. The full band pass of the Al filter is considered, from its cut-on at 17 eV to its cut-off at 73 eV. Due to the lack of experimental data near the cut-on of the filter, the theoretical GDs and reflectivities of the mirrors were used below 20 eV. Above 30 eV, only measured data were used. In the intermediate range the two were averaged to achieve continuity. In the three cases, the pulse durations are reduced resulting in sub-100 as pulses. The reason for such a pulse shortening is that the negative GDD of Al below 35 eV compensates for the intrinsic GDD of the harmonic emission in this spectral range. To be more specific, the combination of the filter and mirrors M_2 or M_3 allows a phase compensation over a large spectral bandwidth that shortens the attosecond pulse down to 85 as, close to the Fourier limit of 74 as. As for M_1, the main peak is followed by replicas of decreasing amplitudes. Identifying the source of such a beating and controlling it through the introduction of a new degree of freedom, namely the angle of incidence on the mirror, make it possible to achieve attosecond pulseshaping, as described below.

5. Controlling sub-100 as beating

By modifying the angle of incidence θ, one controls the spectral phase of the mirror, as exemplified in Fig. 2(a,c). Indeed the accumulated phase through the layers varies as $\cos\theta$, *i.e.* the mirror's response will be highly sensitive around $\theta \simeq 45^\circ$. This turns into a great advantage of these mirrors: when paired together, they form a pulse shaper that may be adjusted simply by turning a rotation stage (inset in Fig. 6(a)). This allows fine control of the GDD above 35 eV. The aluminum filter introduces an important GDD below 35 eV (Fig. 6(b)). By combining the filter and the mirrors, the GDD control can be extended over a larger bandwidth, resulting in shorter attosecond pulses. Alternatively, one can design conditions where the two spectral regions have opposite GDDs, resulting in third-order dispersion (TOD) and attosecond beating, as will be shown below.

Taking as an incoming radiation the harmonic spectrum and GD deduced at the source from "direct" measurements, and using tabulated values for the Al filter response, we calculated the temporal profiles of the pulses outgoing the pulse shaper (Fig. 6(a,c)). In the first configuration, M_1 and M_3 are combined. The pulse reconstructed for $\theta = 42^\circ$ consists of a main 85 as pulse followed by two weak replicas (Fig. 6(a)). Since the experimental results of Fig. 2 showed a

#140608 - $15.00 USD Received 4 Jan 2011; revised 4 Feb 2011; accepted 5 Feb 2011; published 11 Feb 2011

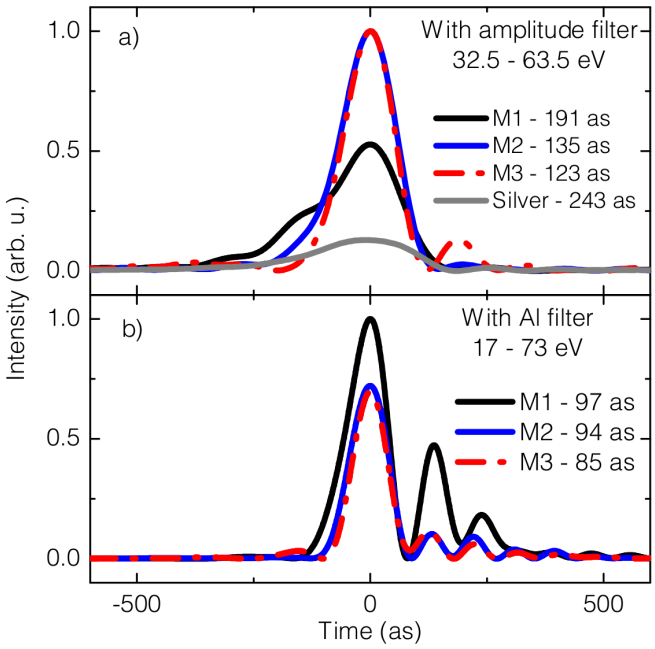

Fig. 5. Temporal reconstruction of attosecond pulses after reflection off the mirrors using the data displayed in Fig. 4 and the corresponding ones for M_1, M_3 and the reference mirror when considering (a) only the 32.5 - 63.5 eV range, or (b) the transmission through a 250 nm-thick aluminum filter. The full width at half maximum is indicated for each pulse.

good agreement with theoretical predictions, we can reliably simulate the behavior of the mirrors for higher incidence angles. Increasing θ makes double sub-100 as pulses appear with variable relative intensities, as reported in Fig. 6(a). Now changing the M_3 mirror for a second M_1-type mirror (2nd configuration), we can extend the tunability to get multiple sub-100 as pulses as exemplified in Fig. 6(c) for $\theta = 52.5°$.

The reason for the observed attosecond beating lies in the phase profiles of the outgoing radiation (Fig. 6(b)). In the 15-35 eV range, which lies close to the onset of the Al transmission, the initial positive GDD is overcompensated by the dispersion of the filter and either brought back towards zero by M_3 or slightly affected by M_1. In the 35-73 eV range, the initial GDD is barely affected by the filter and M_1, but is decreased by M_3, depending on θ. Altogether, the final group delay may then be approximated by two linear zones with slopes of opposite signs and is fitted by a second order polynomial. The highest order corresponds to third-order dispersion (TOD). The TOD value can be adjusted from 3.1×10^5 as^3/rad^2 to 5.7×10^5 as^3/rad^2 by varying the incidence angle and the mirrors. Further insight can be gained in the temporal domain: Fig. 6(c) shows the temporal profiles and instantaneous frequencies, calculated for the two aforementioned spectral ranges in the second configuration. The chirps of the two pulses have opposite signs, following those of the GDDs. The difference in instantaneous frequencies increases with time from $\delta\omega \simeq 15$ eV to $\delta\omega \simeq 42$ eV. It leads to a beating of the coherent sum of the two pulses with a period $T = 2\pi/\delta\omega$ decreasing from 260 as to 100 as. The resulting pulse durations ($\simeq T/2$) nicely match the values in Fig. 6(c). By precisely tailoring the chirp in the different spectral regions, we can thus finely control the attosecond beating.

#140608 - $15.00 USD Received 4 Jan 2011; revised 4 Feb 2011; accepted 5 Feb 2011; published 11 Feb 2011

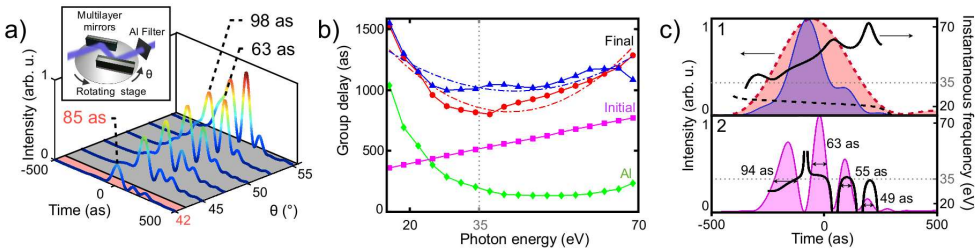

Fig. 6. Attosecond pulse shaping using a tunable pulse shaper based on a rotating pair of multilayer mirrors and an aluminum filter (inset): (a) Temporal profiles obtained using M_1 and M_3 for different angles of incidence θ. The reported durations are the full widths at half maximum. (b) GD curves of the HHG source (purple squares), the Al filter (green losanges), the outgoing radiation from the pulse shaper in the 1st configuration at 42° (blue triangles), in the 2nd configuration at 52.5° (red circles), and the corresponding second order fits for the latter two (dashed-dotted lines) (c) Study of the 52.5° case in (b): temporal profile (shaded curves) and instantaneous frequency (lines) for (1) the 15-35 eV spectral range (dotted lines), and the 35-73 eV range (solid lines), (2) the pulse corresponding to the coherent superposition of the previous pulses.

6. Conclusion

In conclusion, we have manufactured broadband aperiodic multilayer chirped XUV mirrors using a combination of three materials (Mo, Si, B_4C). Utilized with metallic filters, these mirrors allow unprecedented control of the phase and amplitude in a broad XUV spectral range; this results in a variety of attosecond pulse-shaping functions, such as pulse compression and attosecond beating (related to second and third order dispersion), that can be controlled by changing the incidence angle on the mirrors. This opens manyfold perspectives. First it may allow the production of much shorter attosecond pulses than currently available. Indeed, the harmonic plateau extends over hundreds of eV and could sustain pulses much shorter than the atomic unit of time if the intrinsic atto-chirp were properly compensated for. Our phase-controlled mirrors, when combined with the currently used compensation techniques, will allow a phase control over larger bandwidths. Second, the demonstrated pulse shaping opens the possibility of extending coherent quantum control to the extreme ultraviolet and attosecond domains. For instance, coherent transient enhancements of a resonant transition [29] could be induced by adjusting the chirp of the XUV pulse. Finally, a new type of attosecond pump-probe experiments would be made possible by finely controlling the delays between the peaks in the multipulse.

Acknowledgments

We thank S. Nannarone, N. Mahne and A. Giglia for assistance at Elettra Sincrotrone Trieste, T. Auguste and P. Breger for their help on the CEA experiment. We acknowledge financial support from the EU-FP7-ATTOFEL, ANR-09-BLAN-0031-01 and RTRA-Triangle-2008-045T.

#140608 - $15.00 USD Received 4 Jan 2011; revised 4 Feb 2011; accepted 5 Feb 2011; published 11 Feb 2011